Spatial resolution of the HRRT PET scanner using 3D-OSEM PSF reconstruction

Oline Vinter Olesen, Merence Sibomana, Sune Høgild Keller, Flemming Andersen, Jørgen Jensen, Søren Holm, Claus Svarer and Liselotte Højgaard

+

I. Introduction

THE spatial resolution of the Siemens High Resolution Research Tomograph (HRRT) dedicated brain PET scanner [1] installed at Copenhagen University Hospital (Rigshospitalet) was measured using a point-source phantom with high statistics. Further, it was demonstrated how the newly developed 3D-OSEM PSF reconstruction can improve the resolution in reconstructed images with high signal-to-noise-ratios [2], [3].

II. Method

A. Point source

A micro drop of ^{18}F-FDG solution was drawn into the end of a changeable 2ml Pasteur glass pipette or a 20µl capillary tube by capillary forces, and the end was closed by wax. The inner diameter was 0.3-0.7mm, the length of the drop was less than 2mm, and the activity of the drop was 300-800kBq.

B. Scans

The point source was located at different locations within the FOV of HRRT and a 5 minutes emission (EM) scan was acquired on the HRRT for each position. 36 measurements were acquired over three days with four point sources. The locations of the point sources were in the center axial plan (±2mm) with various radii (*r*) and angles (θ) from the center of the transaxial image plane and are shown in Fig. 1.

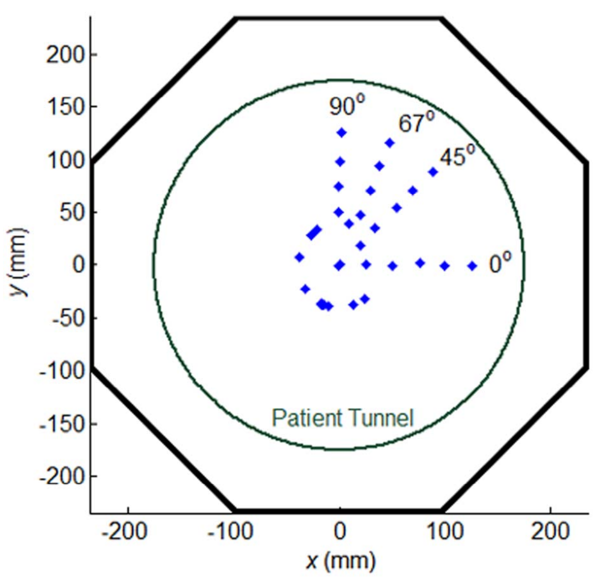

Fig. 1. Transaxial view of the octagonal scanner geometry of the HRRT with blue diamonds indicating the 36 locations at which the point source was scanned (x: left/right, y: anterior/posterior).

C. Reconstruction and Gaussian fit

The 5 minute EM scans were reconstructed using either the ordinary 3D-OSEM algorithm or the improved 3D-OSEM PSF algorithm with resolution modeling in the image space. Both algorithms were run with 16 subsets and 6 iterations. A zoom factor of 5 was used to decrease the size of the reconstructed voxels from 1.22mm to 0.24mm/pixel in the transaxial axes to enable a more precise fit of a Gaussian distribution to the intensity profiles of the principal axes. From these fits the Full Width Half Maximum (FWHM) in the images were determined.

III. Results

The FWHMs for the fitted Gaussian distributions were calculated for the point source in each of the zoomed images reconstructed with and without the PSF modeling. The calculated FWHM of the tangential and radial axes for both reconstructions are shown in Fig. 2. The image and fit for one of the reconstructions with PSF modeling is shown on Fig. 3.

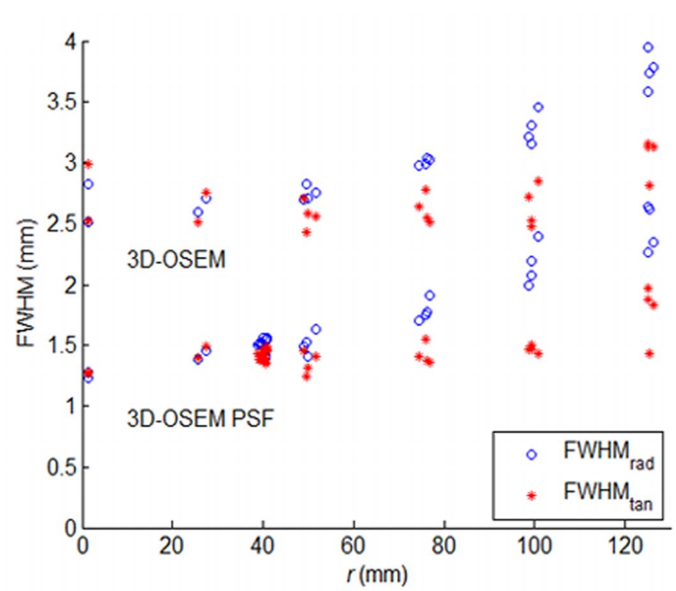

Fig. 2. Plot of the HRRT point source resolution measurements. For all radii the FWHMs of the PSF reconstructions are all significantly lower than the FWHMs of the non-PSF reconstructions.

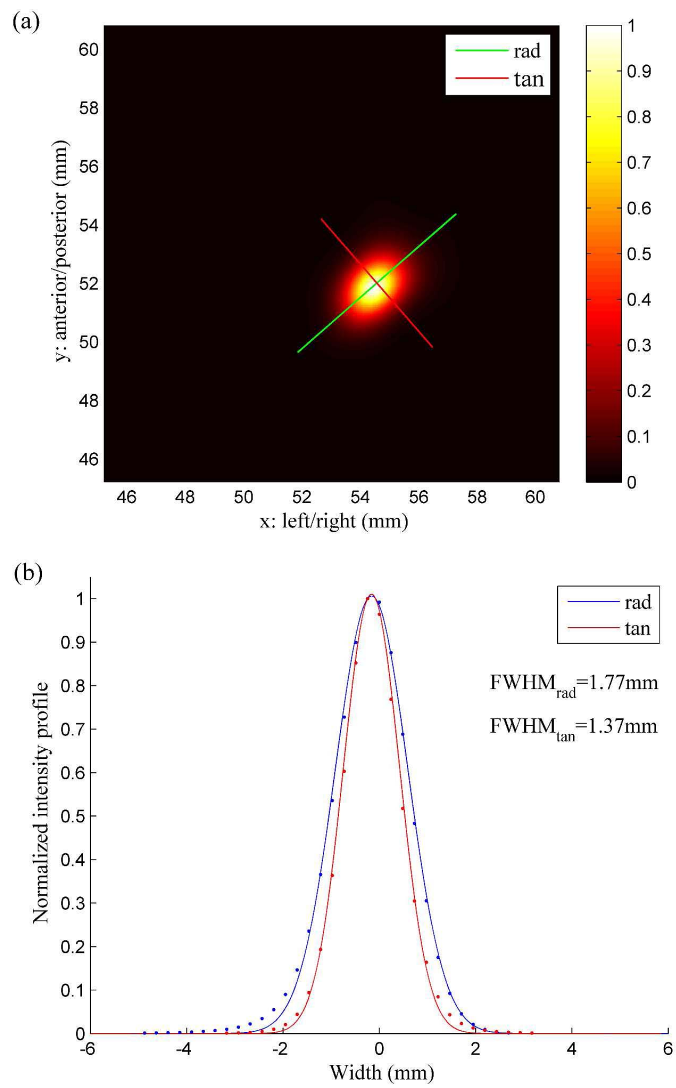

Fig. 3 (a) Axial PET image-slice of the point source r=75 mm and $\theta = 45^{\circ}$, radial and tangential axes plotted on top of the image. (b) Intensity profile along the radial and tangential axes with a fitted Gauss curve for the same point.

A. Resolution and radius

The resolution was significantly improved using the PSF reconstruction. The improvement is 43% ±6% at all distances when comparing the radial and tangential FWHM for the two reconstructions (top and bottom point series in Fig. 2). The

FWHM of both the radial and tangential axis is 1.44 mm ± 0.09mm (n = 46) for $r < 60$mm using the PSF reconstruction. There is a significant difference of only 0.07mm between the radial and tangential FWHM for $r < 60$mm ($p < 10^4$). The radial FWHM decreases with approx. 1mm/85mm when r is above 45mm ($R^2 = 0.90$, n = 16).

B. Resolution and angle

The gaps between detector panels in the octagonal geometry of the HRRT are often a matter of concern in HRRT image reconstruction. There was no significant correlation in resolution with the gaps of the detector panels. The FWHMs measured at $\theta = 67.5^{\circ}$ where the point sources were placed in the detector gaps were not significantly higher than the FWHMs measured at angles 0°, 45° and 90° where the point sources were located orthogonally to the detector panels.

There was a significant difference between the measurements at different angles ($p = 0.015$) for $r > 50$mm: The resolution measurements at $\theta = 90^{\circ}$ were significant higher than the measurements at angles 0°, 45° and 67.5° (p = 0.004-0.045). The scans were done over three different days with four different point sources, which may explain the difference for the scans at $\theta = 90^{\circ}$ done with one of the point sources.

IV. Conclusion

The resolution of the HRRT is centrally ($r < 60$ mm) homogenous with a FWHM of 1.4mm for ^{18}F-FDG in air. This is where the main part of the brain is located if the patient has been positioned correctly. The 1.4mm resolution is obtained using the newly develop 3D-OSEM PSF reconstruction algorithm, which is a significant improvement over 3D-OSEM reconstruction *without* PSF. The algorithm uses a simple PSF model that is the same for all the pixels in the FOV and does not regulate for the circular/octagonal scanner geometry. This supports that the FWHM of the radial axis is increasing with the distance from the center for $r > 60$mm.

References

[1] K. Wienhard *et al.*, The ECAT HRRT: performance and first clinical application of the new high resolution research tomograph, *IEEE Trans. Nucl. Sci.*, vol. 49, pp.104-110, 2002.

[2] C. Comtat *et al.*, Image based resolution modeling for the HRRT OSEM reconstruction software, IEEE MIC Record, Dresden, 2008.

[3] F.C. Sureau, A.J. Reader, C. Comtat, C. Leroy, M.-J. Ribeiro, I. Buvat, and R. Trébossen, *Impact of Image-Space Resolution Modeling for Studies with the High-Resolution Research Tomograph, JNM***49** (2008), 1000-1008